Experimental Investigation of Flow Regimes of Axisymmetric and Planar Opposed Jets

Wei-Feng Li, Tian-Liang Yao, Hai-Feng Liu, and Fu-Chen Wang
Key Laboratory of Coal Gasification of Ministry of Education, East China University of Science and Technology, Shanghai 200237, China

DOI 10.1002/aic.12369
Published online August 31, 2010 in Wiley Online Library (wileyonlinelibrary.com).

Dynamic behaviors of axisymmetric and planar opposed jets have been experimentally studied at 786 < Re < 6288. The flow patterns were investigated by a smoke-wire technique, and the smoke-wire photos were recorded by a high-speed camera. Different flow regimes of axisymmetric and planar opposed jets have been identified. Axisymmetric opposed jets exhibit axial quasi-periodic oscillations, stagnation point offsets, and steady states, while planar opposed jets exhibit both horizontal instabilities and deflecting oscillations. Effects of the nozzle separation and the exit Reynolds number on the dynamic characteristics of axisymmetric and planar opposed jets have been investigated and discussed. Maps of parameter spaces describing the flow regimes of axisymmetric and planar opposed jets at various nozzle separations and exit Reynolds numbers have been presented. © 2010 American Institute of Chemical Engineers *AIChE J,* 57: 1434–1445, 2011

Keywords: axisymmetric and planar opposed jets, fluid mechanics, visualization, oscillation, flow regime

Introduction

Impinging streams (IS) is a unique and multipurpose technique, which can intensify transfer and mixing processes effectively. The technique was first proposed by Elperin and further developed by Tamir.[1,2] On the basis of extensive studies, Tamir concluded that almost all processes in the chemical engineering can be carried out by IS technique, presumably with a higher efficiency in comparison with conventional methods. In the last 20 years, the opposed jets have been widely and successfully applied to a number of industrial processes including reaction injection molding (RIM),[3–7] confined impinging-jets reactors (CIJR),[8–10] absorption,[11–13] opposed multiple burners (OMB) coal gasification,[14,15] etc. Opposed jets have become an increasingly important technique to the chemical industry. Nevertheless, the fundamental study of opposed jets is still very limited and imperfect in comparison with the classic flows, such as jets and wakes.

Opposed jets have been applied with various nozzle separations and exit Reynolds numbers. For example, opposed jets of $L < 2D$ are used to study chemical kinetics and ignition/extinction of diffusion and premixed flames; opposed jets of $L = 4.76D$ are used in CIJR to obtain high mixing efficiency[9]; $L = 10.67D$ and low Re are used in the RIM for the production of polymer[3]; large nozzle separations ($L > 12D$) and high Re are adopted in the OMB gasifier to avoid the ablation of the high temperature flame to the reactor wall.[15] Most previous studies on opposed jets are at specified nozzle separations and exit Reynolds numbers, and there are some discrepancies of the results of the studies.

The study of flow regimes of opposed jets is very important to the design and operation of impinging-jets reactors. Instabilities of opposed jets have been observed by many researchers at various nozzle separations, exit Reynolds numbers, and nozzle types in their experiments but evidently

Correspondence concerning this article should be addressed to W.-F. Li at liweif@ecust.edu.cn.

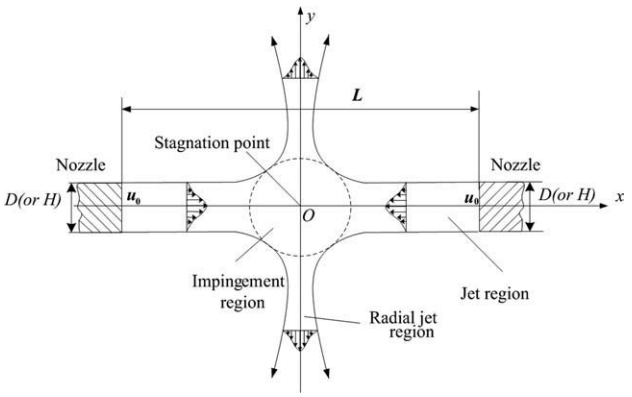

Figure 1. Schematic plan of opposed jets.

different types of unstable behaviors have been reported. The flow regimes in the literature are summarized as follows:

(i) For opposed jets in confined chambers, such as RIM or CIJR, the impingement plane is distorted and shows a sustainable and chaotic flow regime.[3–7] A similar conclusion of these studies is that there exists a critical *Re* in the range of 50–100, in which occurs the flow-field transition from stable laminar to unstable oscillation. Johnson[16,17] studied flow characteristic of unequal laminar opposed jets in RIM numerically. He found that unequal flow rate ratios alter the flow field significantly by moving the impingement point toward the lower momentum jet and stabilize the flow field to some extent. For axisymmetric opposed water jets in the tank, Stan and Johnson,[18] and Zhao and Brodkey[19] observed an irregular oscillation with a low frequency ($\sim$1 Hz). The flow regime in the confined chamber is mainly caused by the pressure feedback of the wall and the vortices formed near the impingement point.

(ii) For opposed jets in nonrestrained environment, the main flow regime is the impingement plane offsets from the center.[20–25] Kostiuk et al.[23] observed that it was very difficult to get the stagnation point to locate at the midpoint of the two nozzles at $L = 2D$. In our previous study,[26,27] the stagnation point offset of turbulent axisymmetric opposed jets with $Re > 4500$ has been studied. In the study, an important conclusion is that there exists a range of $2D \leq L \leq 8D$, in which the stagnation point is very sensitive to the exit velocity ratios, and a very slight difference (3% or less) of exit velocities can cause the stagnation point to deviate from the center dramatically. Ciani et al.[25] and Pawlowski et al.[28] performed simulations and bifurcation analyses of the structure and stability of laminar axisymmetric opposed jets. Their simulations show that axisymmetric opposed jets with identical mass flow rates exhibit multiple steady states at $Re > 60$.

(iii) For planar opposed jets, Denshchikov et al.[29,30] experimentally observed a deflecting oscillation and opposed jets were deflected in the opposite directions from each other and switched directions periodically. Later, several simulations have been performed about the mixing and flow characteristics of two-dimensional confined opposed jets. Hosseinalipour and Mujumdar[31,32] and Wang et al.[33] have studied the flow and mixing characteristics of equal and unequal planar opposed jets numerically. The 2D simulation of the laminar opposed jets by Devahastin and Mujumdar[34] shows that there is a transition from steady state to oscillation (periodic or random oscillatory) and the transition Reynolds number depends strongly on the geometric configuration. The simulation of Pawlowski et al.[28] shows that planar opposed jets with identical mass flow rates exhibit multiple steady states and, in certain cases, periodic steady states.

Because of the difference of the nozzle configuration, the exit Reynolds number and the nozzle separation, there are still some discrepancies for the flow regimes and the critical parameter reported by above researchers. Motivated by the contributions of above studies, we present a fundamental study of the flow characteristics of axisymmetric and planar opposed jets with *Re* in the range of 786–6288. Current work is an extension and advancement of our previous studies,[26,27] in which the location of the stagnation point of turbulent axisymmetric opposed jets with unequal exit velocities was investigated and the factors influencing the stagnation point offset were discussed. In this study, we aim to study the dynamics behaviors of axisymmetric and planar opposed jets and discuss the influences of *Re* and nozzle separations on the flow regime.

Experimental Study

Setup

The schematic drawing of the flow of opposed jets is shown in Figure 1. The flow field was obtained by two

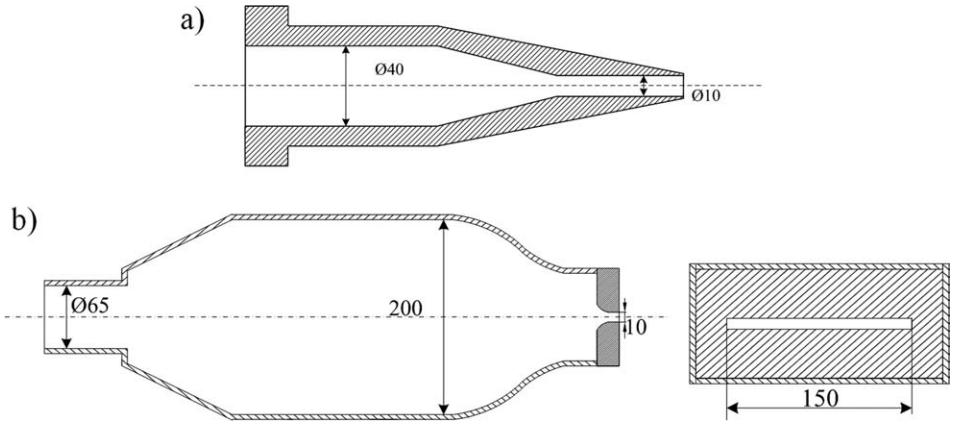

Figure 2. Cross section of axisymmetric (a) and planar (b) nozzles with all dimensions in millimeters.

Table 1. Summary of Experimental Conditions and Parameters

D & *H* (mm)	*L*/*D* & *L*/*H*	u_0 (m/s)	*Re*
10	1, 2, 4, 6, 8, 12, 16, 20	1.18, 2.36, 4.72, 9.44	786–6288

opposed axisymmetric or planar nozzles, as plotted in Figure 2. The two opposing nozzles with same geometric configurations and equal exit velocities were installed in a three-dimensional coordinate frame to adjust the separation (L) and make them coaxial. The exit diameter (D) of the axisymmetric nozzle is 10 mm, and the height (H) and width (W) of the slit of the planar nozzle are 10 and 150 mm, respectively.

The jet Reynolds numbers at axisymmetric and planar nozzle exits are defined as

$$Re = Du_0\rho/\mu, \quad Re = Hu_0\rho/\mu \tag{1}$$

where u_0 is the exit bulk velocity of the jets; ρ and μ are the density and dynamic viscosity of air, which are 1.21 kg/m^3 and 18.1×10^{-6} Pa·s under experimental conditions.

Flow visualization

The instantaneous flow patterns of opposed jets were visualized by a smoke-wire technique, as same to our previous work.[27] Two kinds of stainless steel wires with diameters of 0.076 and 0.154 mm were used. A high-speed camera (Photron, APX-RS) was used to capture the smoke-wire picture with a resolution of 1024 × 1024 pixels. The exposure time was set at 0.001 s and the frame rate was 1000 frames per second. The experimental cases of the flow visualization are listed in Table 1.

The recorded digital images were analyzed with the NIH Image freeware. Because the images were acquired at an interval of 0.001 s, the time series of locations of the impingement planes can be obtained conveniently using the image processing software. Once locations of the impingement planes in two continuous images with an interval of 0.001 s were obtained, the mean movement velocity in this interval can also be calculated. The power-frequency spectra of the time series were obtained by means of fast Fourier transform (FFT).

In the flow visualization, the wake influence of the wire must be considered and minimized. When air flows across the resistance wire, it will induce vortices and oscillations.[35] The local wake *Re* of the resistance wire can be described as

$$Re = du_0\rho/\mu \tag{2}$$

where d is the diameter of the resistance wire; u_0, ρ, and μ are the velocity, density, and dynamics viscosity of air, respectively. At $Re < 40$, the wake is an undetached flow or separated flow with a fixed vortex pair. At $d = 0.076$ mm, the *Re* is in the range of 6–45; at $d = 0.154$ mm, the *Re* is in the range of 11–91; and at $Re > 40$, it will cause vortex streets, which will carry some disturbance into the flow.[35] So, if not specifically stated, the wire diameter is 0.076 mm in this article, and the wire of 0.154 mm is only used for comparison.

Exit velocity profiles of axisymmetric and planar nozzles

The axial mean and root mean square velocity profiles at the exits of the axisymmetric and planar nozzles were measured by a DANTEC hot-wire anemometer. The mean velocity and turbulence intensity profiles of the two types of nozzles are plotted in Figure 3. In the range of $u_0 = 1.18$–9.44 m/s, the exit turbulence intensities of axisymmetric and planar nozzles are about 1 and 3%, respectively. With the increase of *Re*, the exit velocity profile becomes flatter. At $u_0 = 1.18$ m/s, the velocity profile of the axisymmetric nozzle is laminar flow, while at $u_0 = 9.44$ m/s, the profile is corresponding to turbulent flow.

Results and Discussion

Axisymmetric opposed jets

Three flow regimes of axisymmetric opposed jets have been identified and classified into three kinds according to the visualization results. The first is the oscillation regime that occurs mainly at $L/D \leq 2$ and relative high exit velocity. At $L = 2D$, oscillations of the impingement plane were observed, as shown in Figure 4. In the figures, the time is normalized by L/u_0. It can be seen that the impingement

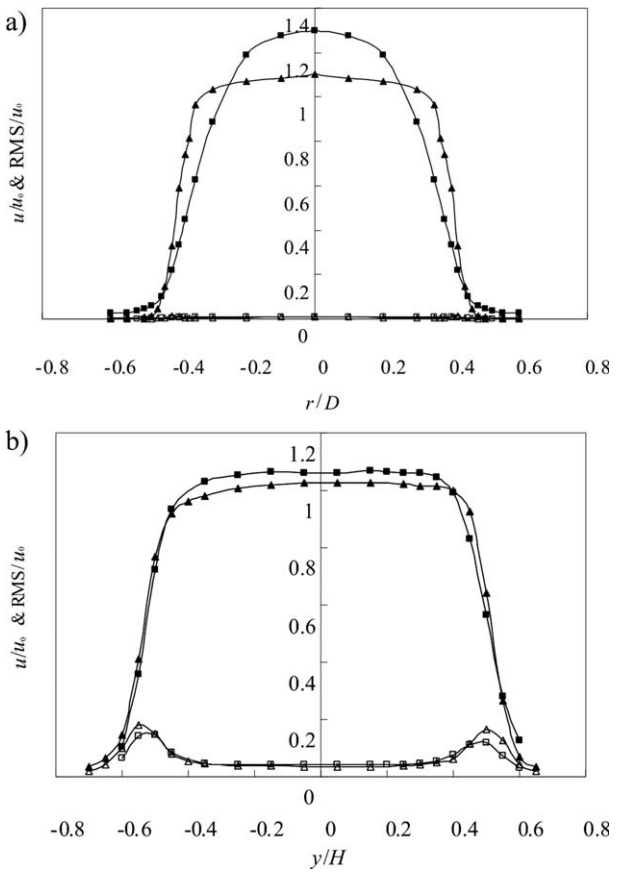

Figure 3. Exit velocity and turbulence intensity profiles of axisymmetric (a) and planar (b) nozzles. ■: mean velocity, u_0 = 1.18 m/s; ▲: mean velocity, u_0 = 9.44 m/s; □: turbulence intensity, u_0 = 1.18 m/s; △: turbulence intensity, u_0 = 9.44 m/s.

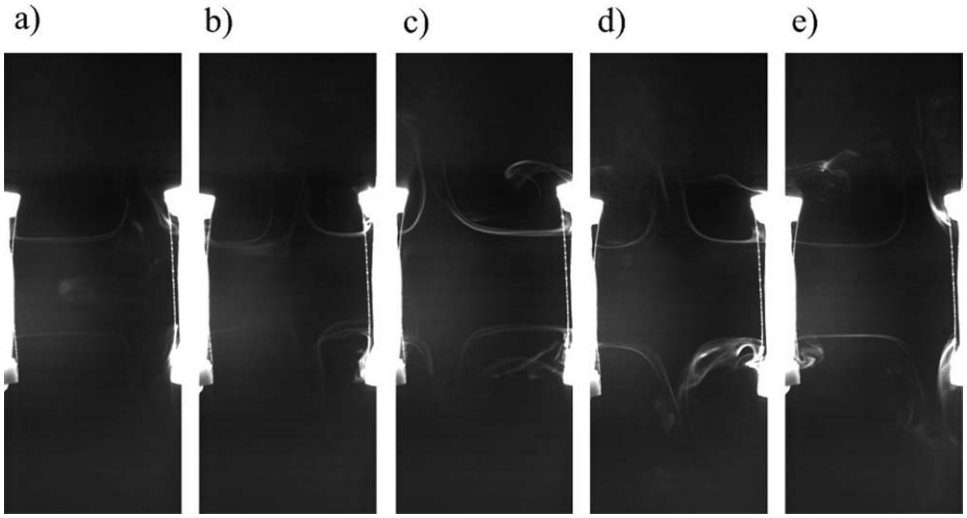

Figure 4. Smoke-wire photos of axisymmetric opposed jets at $L = 2D$ and $u_0 = 4.72$ m/s. (a) $t = t_0$; (b) $t = t_0 + 5.89$; (c) $t = t_0 + 15.31$; (d) $t = t_0 + 22.96$; (e) $t = t_0 + 28.26$.

plane moves back and forth along the x-axis regularly. If T is used to denote an oscillation period, the five photos in the figure approximately correspond to the moments of 0, 1/4T, 1/2T, 3/4T, and T in a full oscillation period. Considering the approximate regularity of the oscillation, we name it the axial quasi-periodic oscillation.

The locations of the impingement plane of axisymmetric opposed jets at $u_0 = 4.72$ and 9.44 m/s were analyzed and plotted in Figure 5. It can be seen that the axial quasi-periodic oscillation appears sometimes, and at other times, the impingement plane oscillates irregularly in a narrow region

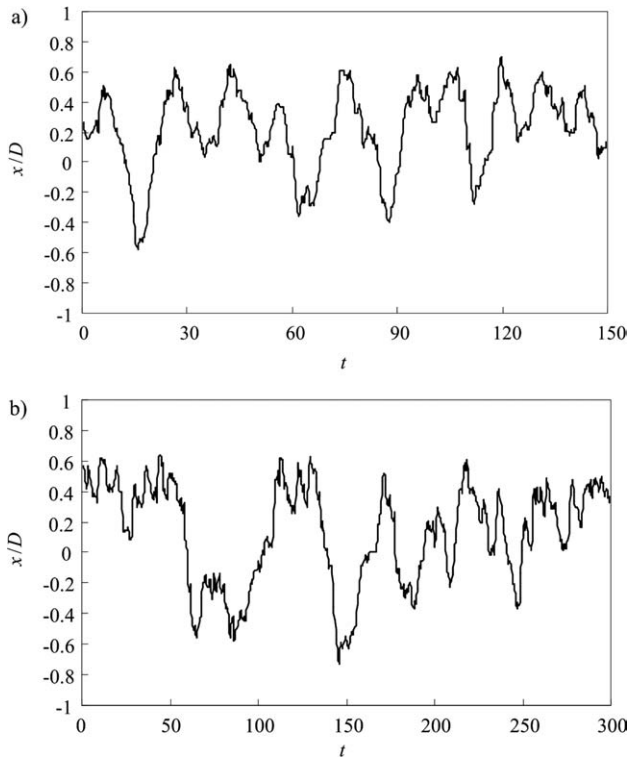

Figure 5. Time series of locations of impingement plane at $L = 2D$, $u_0 = 4.72$ m/s (a) and 9.44 m/s (b).

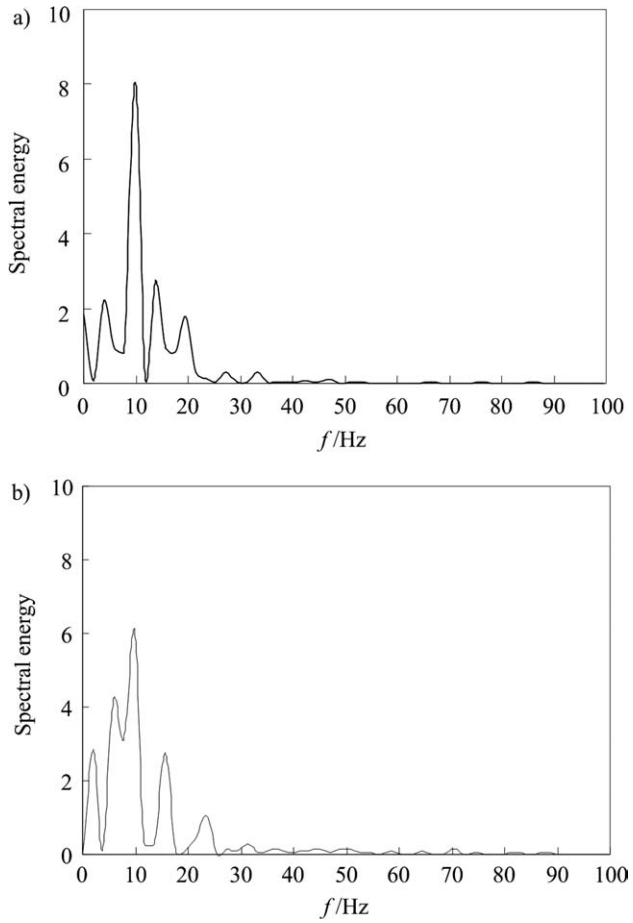

Figure 6. Power-frequency spectra of locations of impingement plane at $L = 2D$, $u_0 = 4.72$ m/s (a) and 9.44 m/s (b).

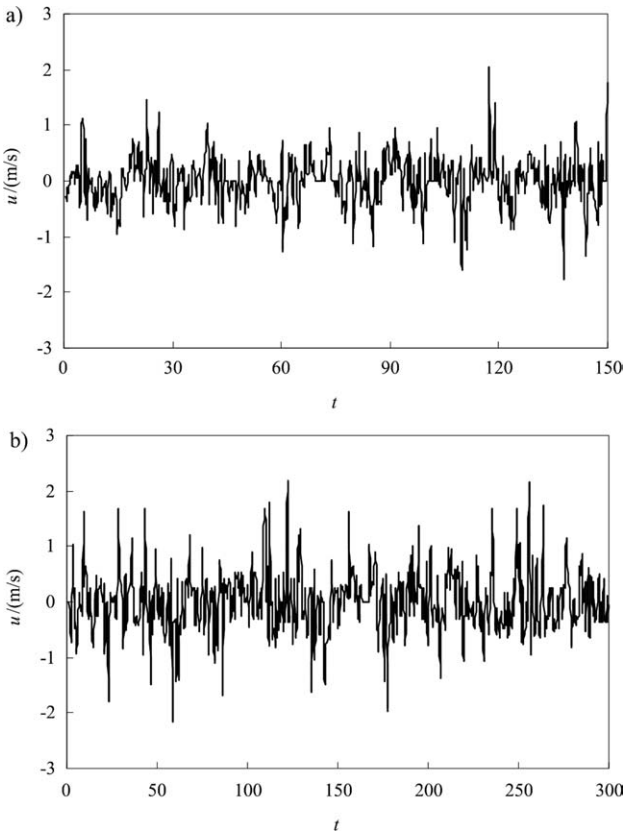

Figure 7. Time series of movement velocity of impingement plane at $L = 2D$, $u_0 = 4.72$ m/s (a) and 9.44 m/s (b).

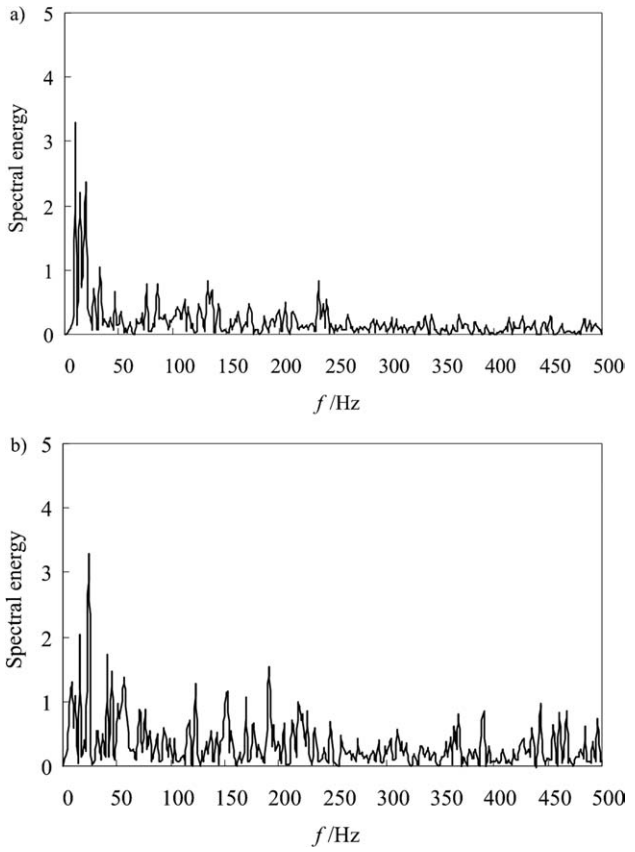

Figure 8. Power-frequency spectra of movement velocity of impingement plane at $L = 2D$, $u_0 = 4.72$ m/s (a) and 9.44 m/s (b).

close to a jet. The power-frequency spectra of the time series of the locations of the impingement planes are shown in Figure 6. In the figures, the x-axis is the oscillation frequency of the impingement plane, and the y-axis is the spectral energy calculated by the square of the FFT modulus. It can be seen from the figure that the oscillation frequency of

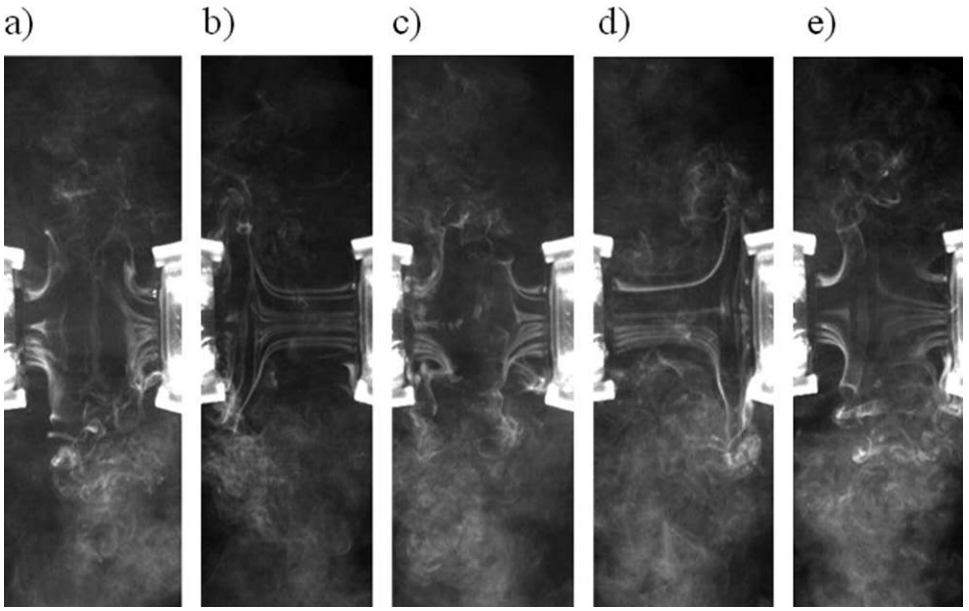

Figure 9. Smoke-wire photos of axisymmetric opposed jet at $u_0 = 2.36$ m/s, $L/D = 2$, and $d = 0.154$ mm. (a) $t = t_0$; (b) $t = t_0 + 3.54$; (c) $t = t_0 + 7.57$; (d) $t = t_0 + 12.98$; (e) $t = t_0 + 15.34$.

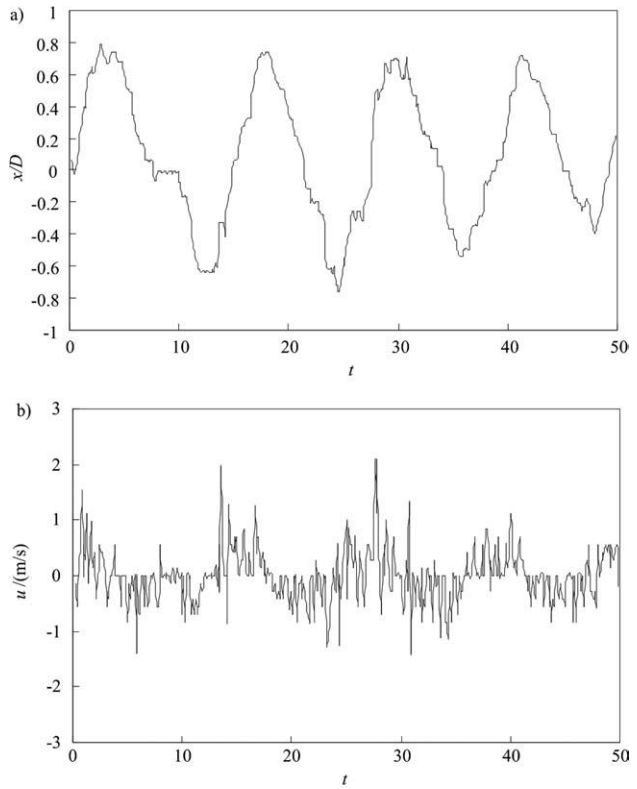

Figure 10. Time series of locations (a) and movement velocities (b) of impingement plane of axisymmetric opposed jets at u_0 = 2.36 m/s, L/D = 2, and d = 0.154 mm.

impingement plane is mainly in the range of 1–30 Hz, and the dominant peaks are about 10 Hz.

The movement velocity of the impingement plane was calculated from the time series of the locations of the impingement planes, as shown in Figure 7. The movement velocity of the impingement plane in the figure is very uncertain and its magnitude varies in the range of 0–2 m/s, which is smaller than the exit velocities of the opposed jets. The power-frequency spectra of movement velocity of impingement plane at u_0 = 4.72 and 9.44 m/s were analyzed and plotted in Figure 8. It can be seen that the dominant peaks appear about in the range of 10–30 Hz, and the power spectra present a large spread of energy around some typical frequency values with the increase of *Re*. As the exit velocity increases from 4.72 to 9.44 m/s, the impingement plane shows a more irregular oscillation, and the oscillation period is more ambiguous, as shown in Figures 5–8.

The oscillation regime reveals that the opposed jets are unstable at close nozzle separations. The irregularity of the oscillation implies that it maybe ascribes to the disturbance. The disturbance could be the fluctuation of the exit flux or turbulence. In the opposed jets, the normal stress in the impingement region is high and increases with decreasing nozzle separation or increasing exit velocity. The fluctuation of the normal stress in the impingement region can also cause the oscillation of the impingement plane. Moreover, although the diameters of the resistance wire and the oil drop are very fine, they still cause some disturbance to the flow. With increases of nozzle separations, the influence of the disturbance caused by the resistance wire and the oil drop decays gradually.

The induced frequency f_s by the resistance wire at the exit can be estimated by

$$f_s = S_t u_0 / d \tag{3}$$

where S_t is the dimensionless Strouhal number; u_0 and d are the air velocity and the diameter of the resistance wire, respectively. For the resistance wire of d = 0.076 mm in current experiment, the Strouhal number is about 0.1 when the wake Reynolds number is in the range of 6–60.[35] The f_s calculated by Eq. 3 is three orders of magnitude larger than the oscillation frequency of the impingement plane, which implies the oscillation induced by the resistance wire is not the direct cause of the oscillation. However, this disturbance excites or intensifies the oscillation of the impingement plane to a certain degree.

Flow patterns of axisymmetric opposed jets with the resistance wire of d = 0.154 mm also have been investigated for comparison. Visualization results show that the flow is more unstable than the 0.076 mm one, and a periodic oscillation happens at $L/D \leq 2$. The smoke-wire photos at L/D = 2 and u_0 = 2.36 m/s are shown in Figure 9. The time series of the locations and the movement velocities of impingement plane are shown in Figure 10. It can be seen that a regular periodic oscillation can be observed and the

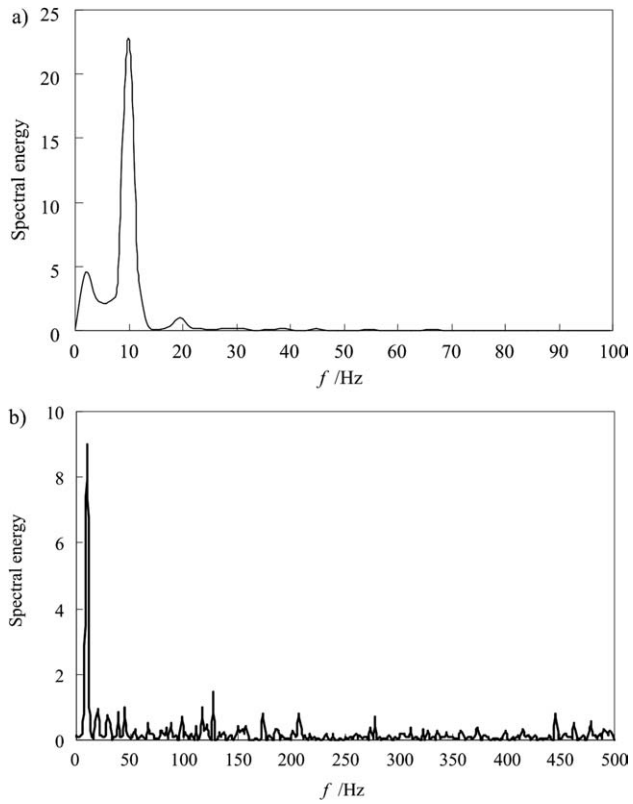

Figure 11. Power-frequency spectra of locations (a) and movement velocities (b) of impingement plane at L = 2D, u_0 = 2.36 m/s, and d = 0.154 mm.

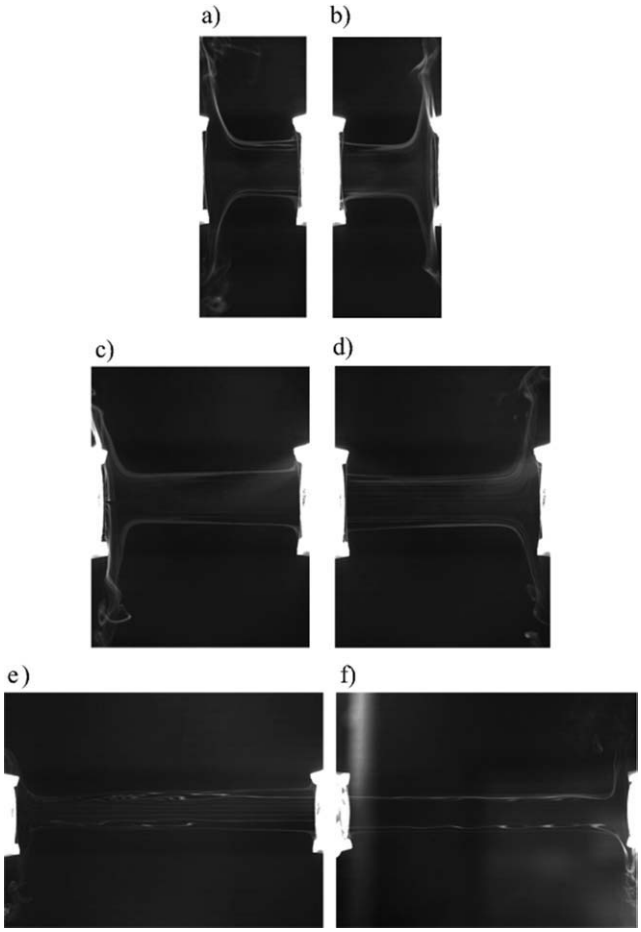

Figure 12. Smoke-wire photos of axisymmetric opposed jets at u_0 = 1.18 m/s, L/D = 2 (a, b), 4 (c, d), and 8 (e, f).

movement velocity of the impingement plane is still in the range of −2 to 2 m/s. The power-frequency spectra of the locations and the movement velocities of the impingement plane are shown in Figure 11. It can be seen that the frequency of the periodic oscillation is about 10 Hz. More results show that the frequency of this periodic oscillation increases with the exit velocity but decreases with the nozzle separation. The periodic oscillation further proves that the flow regime of axisymmetric opposed jets at $L/D \leq 2$ is subject to external disturbance to a large extent.

At $L/D > 2$, one can observe that the impingement plane stays at the positions close to either nozzle exit but it is very difficult to get the stagnation point at the center, as shown in Figure 12. The flow regime is different to the axial quasi-periodic oscillation and we name it the stagnation point offset. More discussion about stagnation point offset of the turbulent opposed jets can be found in our previous work.[26,27]

It should be noted that the two flow patterns at each nozzle separation (e.g., Figures 12a, b) are not interchangeable automatically. However, if we add a little flux to the weaker jet, the sudden switch of the flow patterns will occur. In the experiment, we also find that if we move the hand or other objects fast from the exit of the weaker jet to the stronger jet, the switch of the flow patterns can also happen.

The third flow regime is the steady state, with which the impingement plane can stay at the center when the exit velocities of the opposed jets are equal. Under current experimental cases, the steady state can only be observed at $L/D > 8$, and the impingement plane becomes more and more steady with the increase of nozzle separations. It must be mentioned that this steady state is relative, and when there is a slight difference of the exit velocities, the stagnation plane will move to the weaker jet, especially in the range of L/D = 8–12.

The sketch of the locations of impingement planes at L/D = 1–20 is plotted in Figure 13. In the figure, the height of the arrow denotes the oscillation amplitude; the dot indicates the stagnation point offset; and the square represents the steady state. It is interesting to see that about at L/D = 2–8, the stagnation point offset nearly reaches to the nozzle exit. It must be mentioned that as the stagnation point offset happens, the oscillation still exits but its amplitude is small (less than 1D). As Re increases from 786 to 6288, the flow regimes alter largely. For Re = 6288, the flow becomes stable at L/D = 8–12, and the offset degree decreases at L/D = 4–6, but the oscillation occurs at L/D = 2.

From above discussion, it can be summarized that there are three different flow regimes for axisymmetric opposed jets. The first is characterized by the oscillation behavior; the second corresponds to the stagnation point offset; and the third is a symmetric steady state. Based on more experimental results, the map of the parameter space describing the

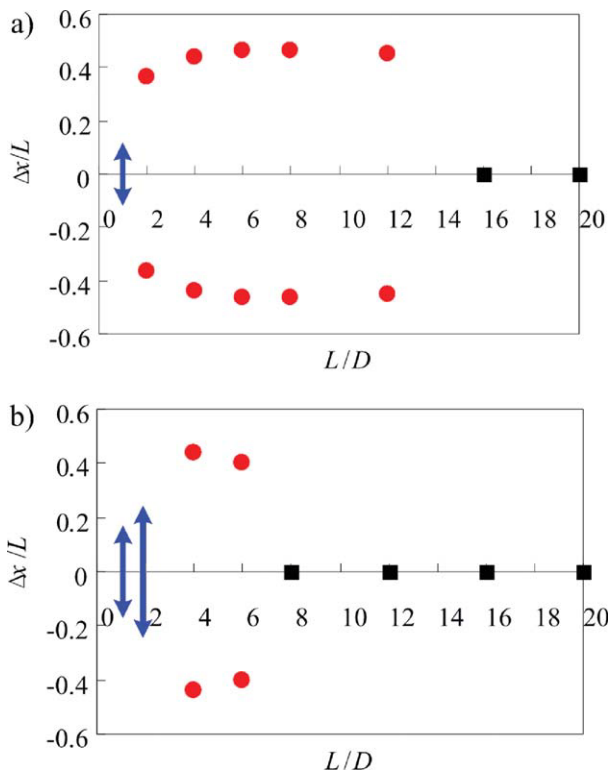

Figure 13. Schematic map of flow regimes of axisymmetric opposed jets at u_0 = 1.18 m/s (a) and 9.44 m/s (b).

[Color figure can be viewed in the online issue, which is available at wileyonlinelibrary.com.]

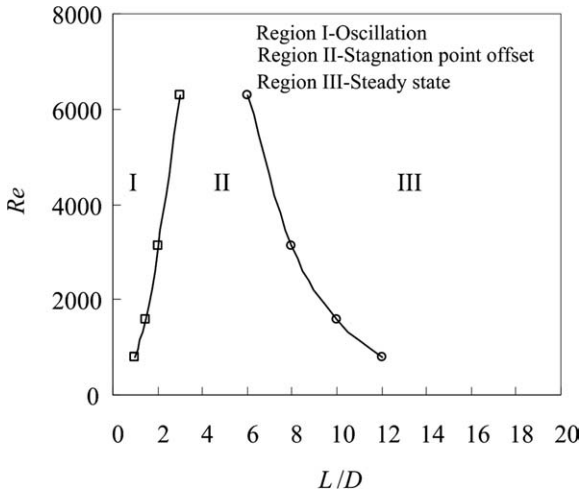

Figure 14. Map of parameter space of flow regimes of axisymmetric opposed jets.

flow regimes of axisymmetric opposed jets is plotted in Figure 14. To be more precisely, the flow regime in the Region I is a hybrid of the axial quasi-periodic oscillation and the stagnation point offset.

Compared with our previous work,[26,27] current results indicate that the stagnation point offset at low *Re* is more remarkable, which implies that *Re* has significant effects on flow regimes of axisymmetric opposed jets. The effect of *Re* on opposed jets is related to the effect of *Re* on the round jet. Many researchers have studied the instability evolution of low *Re* round jet.[36,37] They have observed that as *Re* increases up to about 1000, the jets show the transition from helical instability to axisymmetric instability. Our visualization results show that at $Re < 1000$, the jets are helical and only very small vortices can be observed in the edge of the jet boundary, as shown in Figure 12. However, with the increase of *Re*, the jets change to axisymmetric instability and large-scale vortices appear in the jet boundary. Results indicate that when two low *Re* jets with helical instabilities impact oppositely, the impingement plane is very unstable, while for two jets with higher *Re*, the impingement plane becomes stable comparatively.

Planar opposed jets

From the visualization records, the flow regimes of planar opposed jets can be classified into the horizontal instability and the deflecting instability. At $L/H < 5$, the impingement plane of planar opposed jets stays at the center and oscillates irregularly along the *x*-axis occasionally, as shown in Figure 15. When there is a slight difference of the exit velocities, the stagnation point will move to the position very close to the weaker jet. The flow regime of planar opposed jets at $L/H < 5$ is similar to the axial instability of axisymmetric opposed jets, so we call it the horizontal instability.

For planar opposed jets, another feature is the thickness of the radial jet is bigger than that of axisymmetric opposed jets. As shown in Figure 16, the thickness of the radial jet is about $2H$; however, the thickness of the radial jet of axisymmetric is less than $1D$, as shown in Figure 4. Because the impingement planes of axisymmetric and planar opposed jets are very unstable, measuring the axial velocity distribution is very difficult. So we carried out numerical simulations, and the detailed method of the simulation can be found in our previous paper.[26] The simulation is verified by the analysis solution of Champion and Libby,[38] which is presented for the turbulence flow issuing from two closely opposed jets with uniform exit velocity profiles. According to the analytic solution, the axial velocity distribution of planar opposed jets is described as

$$u = u_0 \sin\left(\pi \frac{x}{L}\right), \qquad -H < x < H \tag{4}$$

where u_0 is the exit bulk velocity and x is the horizontal coordinate.

At $L/H = 1$ and 2, the horizontal velocity distributions using the simulation and analytic solution are shown in Figure 16a. One can see that the two curves are in good agreement. At $L/H = 4$, simulations of the horizontal velocity and

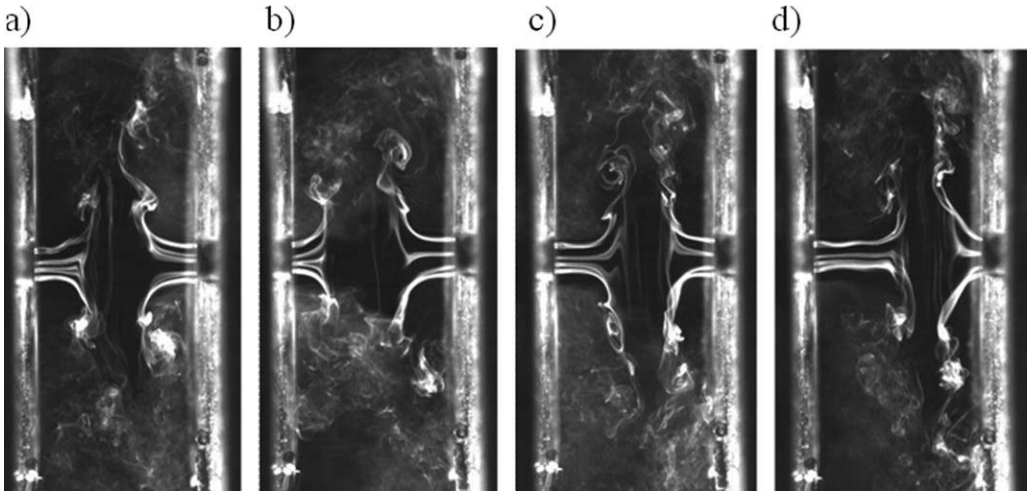

Figure 15. Smoke-wire photos of planar opposed jets at u_0 = 2.36 m/s and L/H = 4. (a) $t = t_0$; (b) $t = t_0 + 14.57$; (c) $t = t_0 + 17.46$; (d) $t = t_0 + 23.19$.

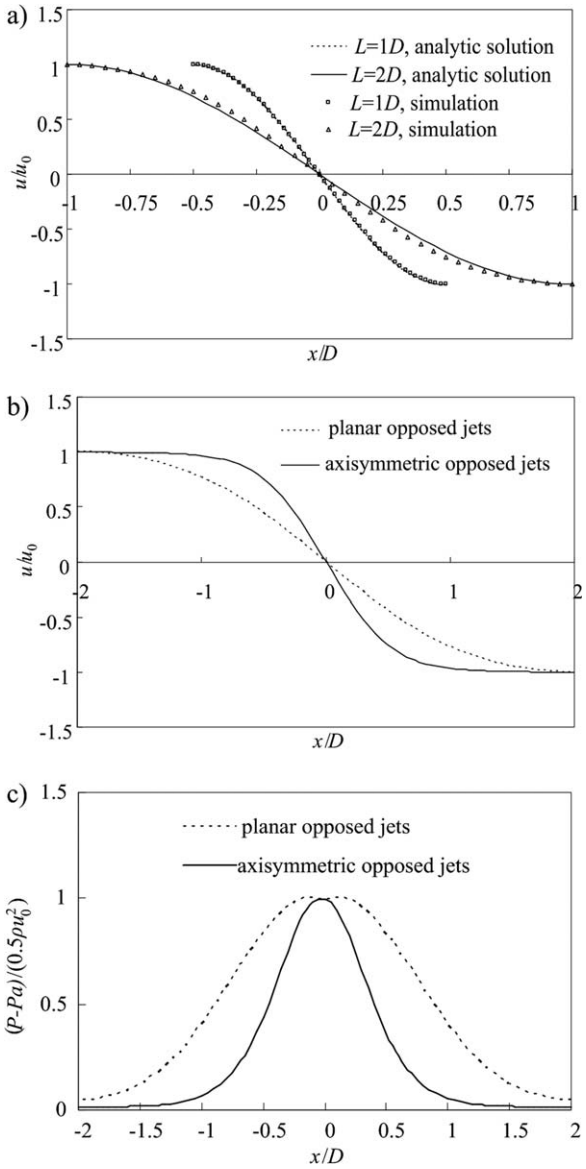

Figure 16. Simulations of horizontal velocity and static pressure distributions. (a) $L/H = 2$, horizontal velocity of planar opposed jets; (b) $L/D = 4$, $L/H = 4$, axial (or horizontal) velocity distributions; (c) $L/D = 4$, $L/H = 4$, pressure distributions.

static pressure of axisymmetric and planar opposed jets are shown in Figures 16b, c. It can be seen that although the max static pressures in the stagnation point of both the opposed jets are equal to $0.5\rho u_0^2$, the pressure region of planar opposed jets are wider than that of axisymmetric opposed jets. The magnitude and direction of the static pressure in the impingement region are relevant to the instabilities of opposed jets.

At $L/H \geq 6$, another flow regime arises, which is characterized by deflecting oscillation. As shown in Figure 17, each planar jet is ''pushed away'' in the opposite direction from the other and periodically switches directions. Compared with the oscillations of axisymmetric opposed jets at $L/D \leq 2$ or planar oppose jets at $L/H < 5$, the deflecting oscillation at $L/H \geq 6$ is more regular.

At $4 < L/H < 6$, planar opposed jets are in the transition from the horizontal oscillation to the deflecting oscillation. As shown in Figure 18, the flow patterns show the horizontal oscillation and the deflecting oscillation at different times alternately. So, $L/H = 5$ is the critical parameter of the two kinds of flow regimes at $Re = 1572$.

The mean period (T) and its standard deviation (S) of the deflecting oscillation are calculated based on 10 sets of data and the results are shown in Figure 19. The figure reveals that the oscillation period at specified condition is almost fixed. The oscillation periods at various nozzle separations and Re are presented in Figure 20. One can see that the oscillation period increases with nozzle separations but decreases with Re.

Compared with the results of Denshchikov et al.,[29,30] the period of the deflecting oscillation in current experiment (0.1–1 s) is of an order of magnitude smaller than theirs (2–30 s). This is due to the fact that the water velocity in their experiment is about of an order smaller than air velocity in our experiment. It is interesting to see in Figure 20b that the normalized oscillation period $T/(L/u_0)$ is about equal to 6, especially at $L/H > 6$ and $Re > 2000$, which is in agreement with Denshchikov et al.[29,30] They deduced the description of the oscillation period using dimensional analysis. We further deduced the final formula of normalized period from their analysis

$$\frac{T}{(L/u_0)} = \sqrt{L/H} \tag{5}$$

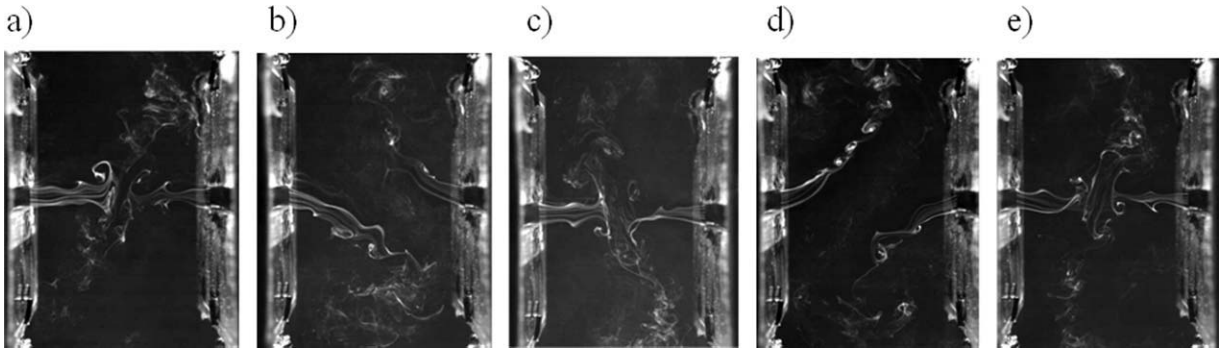

Figure 17. Smoke-wire photos of planar opposed jets at $u_0 = 2.36$ m/s and $L/H = 8$. (a) $t = t_0$; (b) $t = t_0 + 1.86$; (c) $t = t_0 + 3.16$; (d) $t = t_0 + 4.78$; (e) $t = t_0 + 6.31$.

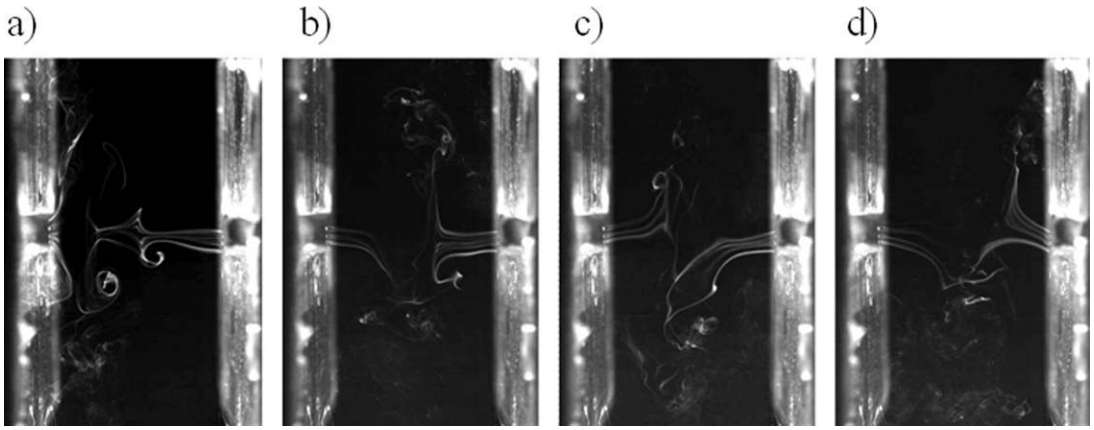

Figure 18. Smoke-wire photos of planar opposed jets at u_0 = 2.36 m/s and $L = 5H$. (a) $t = t_0$; (b) $t = t_0 + 6.84$; (c) $t = t_0 + 11.09$; (d) $t = t_0 + 15.81$.

However, we find Eq. 5 cannot predict our experimental results well. We fitted the normalized oscillation period $T/(L/u_0)$ using nondimensional parameters Re and L/H, and found all the period values could be well described as

$$\frac{T}{(L/u_0)} = 6Re^{0.064}(L/H)^{-0.21} \tag{6}$$

Equation 6 indicates that Re has weak influence on the normalized oscillation period. The main difference between Eqs. 5 and 6 is the exponent of L/H, which maybe ascribes to the difference of the experiment equipment.

According to Johnson and Wood[4] and Teixeira et al.,[5] the Strouhal number describing the oscillation frequency of opposed jets in RIM can be defined as

$$S_t = fD/u_0 \tag{7}$$

where f is the oscillation frequency; u_0 and D are the exit air velocity and the nozzle diameter, respectively. The Strouhal numbers of planar opposed jets calculated by Eq. 7 and the reported values in the literature are shown in Figure 21. The Strouhal number of planar opposed jets is in the range of 0.01–0.03 and is independent of Reynolds number but decreases with increasing nozzle separation. Although the nozzle geometry and boundary condition are different, the Strouhal number of planar opposed jets is nearly on the same level as that in RIM. However, the Strouhal number of planar opposed jets is an order of magnitude less than that of the wake of the cylinder (about 0.1–0.2). If we use the nozzle separation L to define the Strouhal number as

$$S_t = fL/u_0 \tag{8}$$

we find the values the Strouhal numbers of planar opposed jets are in the range of 0.1–0.2, which is similar to the wake of the cylinder.

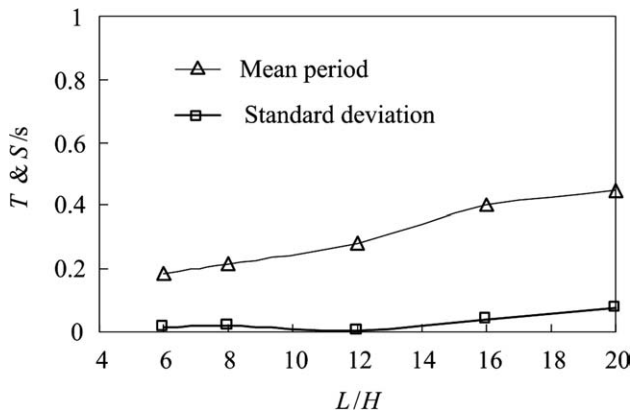

Figure 19. Periods and their standard deviations of planar opposed jets at u_0 = 2.36 m/s.

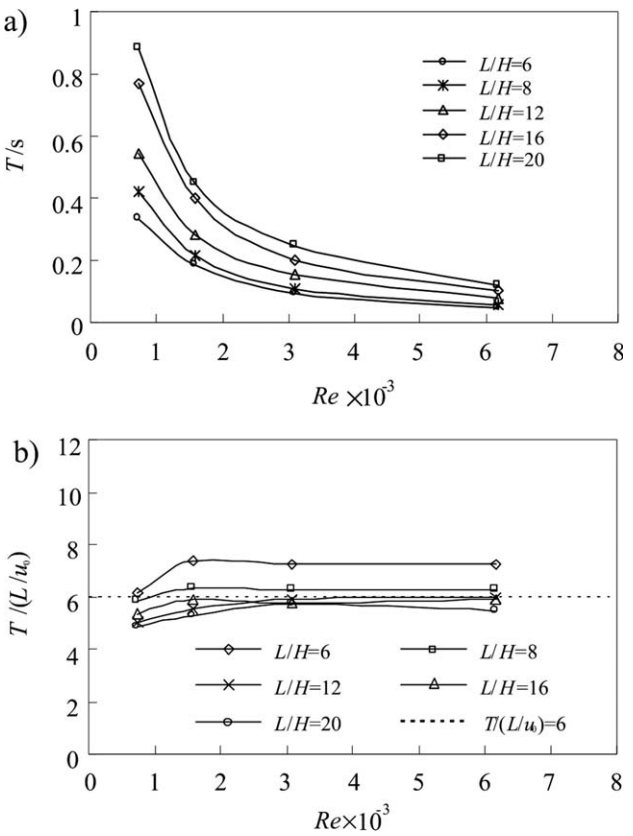

Figure 20. Oscillation periods of planar opposed jets.

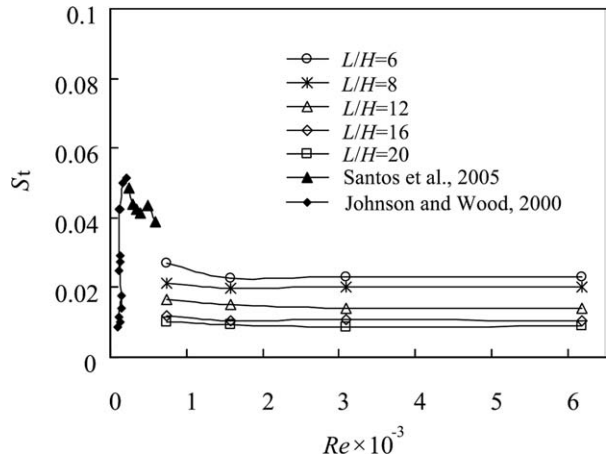

Figure 21. Strouhal number of planar opposed jets at various Reynolds numbers and nozzle separations.

The parameter space describing the flow regimes of planar opposed jets is drawn in Figure 22. Compared with the experimental results of Denshchikov et al. ($100 < Re < 4800$)[29,30] and the simulations of Pawlowski et al. ($1 < Re < 1500$),[28] the transitional nozzle separation from the horizontal oscillation to the deflecting oscillation in this study ($L/H = 5$) coincides with the former ($L/H = 4$–6) but is smaller than the latter ($L/H = 8$–10). The difference between the experiment and the simulations ascribes to the difference of *Re* or boundary conditions.

Discussion

For axisymmetric opposed jets, the axial quasi-periodic oscillation occurs at $L/D \leq 2$ and has not a regular period, while the flow pattern still keeps axisymmetric. The axial quasi-periodic oscillation can be converted to the periodic oscillation when the external disturbance to the system increases. At $L > 2D$, the stagnation point offset replaces the oscillation and becomes the dominant flow regime of axisymmetric opposed jets.

Because of the differences of the nozzle configurations, exit Reynolds numbers and nozzle separations, a quantitative comparison to the published work is difficult. Generally, the finding in this study is in agreement with the observations stated in the Introduction.[20–25] The simulation and stability analysis of Pawlowski et al.[28] show that laminar axisymmetric opposed jets exhibit multiple steady states at $Re > 60$ but no oscillation has been found. The discrepancy is due to the boundary condition difference between the experiment and the simulation, because the external disturbance always exists in experiments.

For planar opposed jets, the periodic deflecting oscillation occurs at $L/H > 5$ and the flow patterns lose their axisymmetry. The deflecting oscillation is a kind of self-sustained oscillation whose period is regular and determined by the system itself. We speculate the deflecting oscillation is caused by the following factors: (i) the two-dimensional nozzle configuration, (ii) the normal stress distribution in the impingement region, and (iii) the instability of large-scale vortices in the jet boundaries.

Hydrodynamics and instabilities of axisymmetric opposed jets in RIM and CIRJ have been studied by many researchers. In these studies, impingement plane was distorted and the large-scale, three-dimensional oscillations were observed. This flow regime is induced by the reactor wall effect and is different to this study. In the literature, there are many comparisons about the oscillation frequency and flow regimes between the confined axisymmetric opposed jets and the planar opposed jets. It must be mentioned that these two kinds of oscillations are different in nature.

Conclusions

To successfully exploit opposed jets for engineering applications, it is important to identify the flow regimes and critical parameters. In this study, the flow regimes of axisymmetric and planar opposed jets were identified and discussed. Results show that opposed jets are unstable, and geometry configurations and *Re* have substantial influences on their flow regimes. The main conclusions are drawn as follows:

(i) The flow regimes of axisymmetric opposed jets are the axial quasi-periodic oscillation, the stagnation point offset, and the steady state. The axial quasi-periodic oscillation occurs at $L/D \leq 2$ and is subject to external disturbance. The stagnation point offset mainly happens in the range of $2 < L/D < 8$, and with the increase of *Re*, the range becomes narrow and the offset degree decreases.

(ii) The flow regimes of planar opposed jets are the horizontal instability and the deflecting oscillation, and $L/H = 5$ is the critical nozzle separation at Re $\approx$ **1000**.

(iii) The axial quasi-periodic oscillation is a kind of destabilization instability; however, the deflecting oscillation is a kind of self-sustained oscillation.

The results in this study represent a significant contribution to the knowledge of flow regimes of axisymmetric and planar opposed jets, which are useful for the design and operation of the reactors with opposed jets. The results will also provide a sound basis for future computational fluid dynamics simulation and stability analysis of opposed jets.

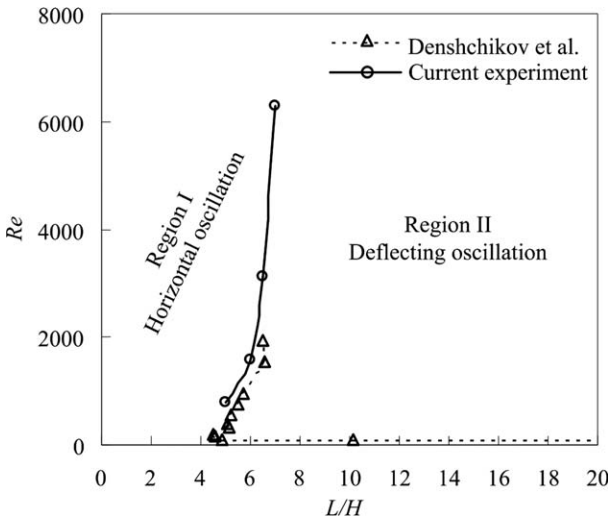

Figure 22. Map of parameter space of flow regimes of planar opposed jets.

Acknowledgments

This study was supported by the National Development Programming of Key Fundamental Researches of China (2010CB227004) and the Natural Science Foundation of China (20906024). Especially, the authors thank the anonymous reviewers for their helpful suggestions on the quality improvement of their article.

Notation

d = wire diameter
D = nozzle diameter
f, f_s = frequency
L = nozzle separation
H = nozzle height
I = turbulence intensity
r = radial coordinate
Re = jet Reynolds number
S = standard deviation
S_t = Strouhal number
t, t_0 = normalized time
T = period
u, u_0 = axial velocity
x, y = axial, radial coordinate
W = nozzle width
ρ = air density
μ = dynamic viscosity of air
Δx = stagnation point offset

Literature Cited

1. Elperin IT. Heat and mass transfer in opposing currents (in Russian). *J Eng Phys*. 1961;6:62–68.
2. Tamir A. *Impinging Streams Reactors: Fundamentals and Applications*. Amsterdam: Elsevier, 1994.
3. Wood PE, Hrymak A, Yeo R, Johnson DA, Tyagi A. Experimental and computational studies of the fluid mechanics in an opposed jet mixing head. *Phys Fluids A*. 1991;3:1362–1368.
4. Johnson DA, Wood PE. Self-sustainable oscillations in opposed impinging jets in an enclosure. *Can J Chem Eng*. 2000;78:867–875.
5. Teixeira AM, Santos RJ, Costa MRPFN, Lopes JCB. Hydrodynamics of the mixing head in RIM: LDA flow-field characterization. *AIChE J*. 2005;51:1608–1619.
6. Santos RJ, Erkoç E, Dias MM, Teixeira AM, Lopes JCB. Hydrodynamics of the mixing chamber in RIM: PIV flow-field characterization. *AIChE J*. 2008;54:1153–1163.
7. Santos RJ, Erkoç E, Dias MM, Lopes JCB. Dynamic behavior of the flow field in a RIM machine mixing chamber. *AIChE J*. 2009;55:1338–1351.
8. Johnson BK, Prud'homme RK. Chemical processing and micromixing in confined impinging jets. *AIChE J*. 2003;49:2264–2282.
9. Liu Y, Fox RO. CFD predictions for chemical processing in a confined impinging-jets reactor. *AIChE J*. 2006;52:731–744.
10. Gavi E, Marchisio DL, Barresi AA. CFD modelling and scale-up of confined impinging jet reactors. *Chem Eng Sci*. 2007;62:2228–2241.
11. Berman Y, Tanklevsky A, Oren Y, Tamir A. Modeling and experimental studies of SO_2 absorption in coaxial cylinders with impinging streams. Part I. *Chem Eng Sci*. 2000;55:1009–1021.
12. Berman Y, Tanklevsky A, Oren Y, Tamir A. Modeling and experimental studies of SO_2 absorption in coaxial cylinders with impinging streams. Part II. *Chem Eng Sci*. 2000;55:1022–1032.
13. Wu Y, Li Q, Li F. Desulfurization in the gas-continuous impinging stream gas–liquid reactor. *Chem Eng Sci*. 2007;62:1814–1824.
14. Higman C, Burgt M. *Gasification*, 2nd ed. Burlington: Gulf Professional Publishing, 2008.
15. Wang FC, Zhou ZJ, Dai ZH, Gong X, Yu GS, Liu HF, Wang YF, Yu ZH. Development and demonstration plant operation of an opposed multi-burner coal-water slurry gasification technology. *Front Energy Power Eng China*. 2007;1:251–258.
16. Johnson DA. Experimental and numerical examination of confined laminar opposed jets. Part I: momentum Balancing. *Int Commun Heat Mass Transfer*. 2000;27:443–454.
17. Johnson DA. Experimental and numerical examination of confined laminar opposed jets. Part II: momentum Imbalance. *Int Commun Heat Mass Tran*. 2000;27:455–463.
18. Stan G, Johnson DA. Experimental and numerical analysis of turbulent opposed impinging jets. *AIAA J*. 2001;39:1901–1908.
19. Zhao Y, Brodkey RS. Averaged and time-resolved, full-field (three-dimensional), measurements of unsteady opposed jets. *Can J Chem Eng*. 1998;76:536–545.
20. Rolon JC, Veynante D, Martin JP. Counter jet stagnation flows. *Exp Fluids*. 1991;11:313–324.
21. Ogawa N, Maki H. Studies on opposed turbulent jets, (Influences of a body on the axis of opposed turbulent jets). *Bull JSME*. 1986;29:2872–2877.
22. Ogawa N, Maki H, Hijikata K. Studies on opposed turbulent jets, (Impact position and turbulent component in jet center). *Int J JSME*. 1992;35:205–217.
23. Kostiuk LW, Bray KNC, Cheng RK. Experimental study of premixed turbulent combustion in opposed streams. Part I-Nonreacting flow field. *Combust Flame*. 1993;92:377–395.
24. Ciani A, Kreutner W, Hubschmid W, Frouzakis CE, Boulouchos K. Experimental investigation of the morphology and stability of diffusion and edge flames in an opposed jet burner. *Combust Flame*. 2007;150:188–200.
25. Ciani A, Kreutner W, Frouzakis CE, Lust K, Coppola G, Boulouchos K. An experimental and numerical study of the structure and stability of laminar opposed-jet flows. *Comput Fluids*. 2010;39:114–124.
26. Li WF, Sun ZG, Liu HF, Wang FC, Yu ZH. Experimental and numerical study on stagnation point offset of turbulent opposed jets. *Chem Eng J*. 2008;138:283–294.
27. Li WF, Yao TL, Wang FC. Study on factors influencing stagnation point offset of turbulent opposed Jets. *AIChE J*. 2010;56:2513–2522.
28. Pawlowski RP, Salinger AG, Shadid JN, Mountziaris TJ. Bifurcation and stability analysis of laminar isothermal counterflowing jets. *J Fluid Mech*. 2006;551:117–139.
29. Denshchikov VA, Kontratev VN, Romashev AN. Interaction between two opposed jets. *Fluid Dyn*. 1978;6:924–926.
30. Denshchikov VA, Kontratev VN, Romashev AN, Chubarov VM. Autooscillations of planar colliding jets. *Fluid Dyn*. 1983;3:460–462.
31. Hosseinalipour SM, Mujumdar AS. Flow and thermal characteristics of steady two dimensional confined laminar opposing jets. Part I. Equal jets. *Int Commun Heat Mass Tran*. 1997;24:27–38.
32. Hosseinalipour SM, Mujumdar AS. Flow and thermal characteristics of steady two dimensional confined laminar opposing jets. Part II. Unequal jets. *Int Commun Heat Mass Tran*. 1997;24:39–50.
33. Wang SJ, Devahastin S, Mujumdar AS. A numerical investigation of some approaches to improve mixing in laminar confined impinging streams. *Appl Therm Eng*. 2005;25:253–268.
34. Devahastin S, Mujumdar AS. A numerical study of flow and mixing characteristics of laminar confined impinging streams. *Chem Eng J*. 2002;85:215–223.
35. Blevins RD. *Flow Induced Vibration*. New York: Van Nostrand Reihold Co., 1977.
36. O'Neill P, Soria J, Honnery D. The stability of low Reynolds number round jets. *Exp Fluids*. 2004;36:473–483.
37. Crow SC, Champagne FH. Orderly structure in jet turbulence. *J Fluid Mech*. 1971;48:547–591.
38. Champion M, Libby PA. Reynolds stress description of opposed and impinging turbulent jets. Part I: closely spaced opposed jets. *Phys Fluids A*. 1993;5:203–216.

Manuscript received Mar. 29, 2010, and revision received Jun. 18, 2010.